объединенный
институт
ядерных
исследований
дубна

E2 - 12605

S.V.Goloskokov, S.P.Kuleshov, O.V.Seljugin

HIGH-ENERGY PROTON-PROTON SCATTERING IN A WIDE MOMENTUM-TRANSFER REGION

1979

E2 - 12605

S.V.Goloskokov, S.P.Kuleshov, O.V.Seljugin

HIGH-ENERGY PROTON-PROTON SCATTERING IN A WIDE MOMENTUM-TRANSFER REGION

Submitted to ЯФ

Голоскоков С.В., Кулешов С.П., Селюгин О.В. **E2 - 12605**

Высокоэнергетическое протон-протонное рассеяние в широкой области передач импульса

Построена модель эйконального типа для амплитуд высокоэнергетического протон-протонного рассеяния, удовлетворяющая требованиям аналитических свойств для амплитуды рассеяния. Модель количественно передает все свойства дифференциальных сечений рассеяния в области энергий $23,4 \le \sqrt{s} \le 62$ ГэВ и передач импульса $0 \le |t| \le 14,2$ ГэВ ^{2}.

Работа выполнена в Лаборатории теоретической физики ОИЯИ.

Препринт Объединенного института ядерных исследований. Дубна 1979

Goloskokov S.V., Kuleshov S.P., Seljugin O.V. **E2 - 12605**

High-Energy Proton-Proton Scattering in a Wide Momentum-Transfer Region

A model of the eikonal type is constructed for the proton-proton scattering amplitude which obeys the requirements of the analyticity properties. The model reproduces quantitatively all properties of the pp differential cross section in the energy range $23.4 \le \sqrt{s} \le 62$ GeV and momentum transfer range $0 \le |t| \le 14.2$ GeV

The investigation has been performed at the Laboratory of Theoretical Physics, JINR.

Preprint of the Joint Institute for Nuclear Research. Dubna 1979

INTRODUCTION

The investigation of high energy elastic scattering processes in a large momentum-transfer region arouses now a considerable interest. This is due to the recent measurement of the proton-proton scattering at ISR [1] and FNAL [2] accelerators. These measurements have revealed the following features of the differential cross sections:

1. The slope of diffraction peak changes near $|t| \sim 0.15$ GeV^2.

2. There is a sharp dip at $|t| \sim$ 1.45 and a wide maximum near $|t| \sim 1.9$ GeV^2, i.e., the differential cross section has a diffraction structure. With growing energy the diffraction minimum and maximum go to the smaller $|t|$ values. At the same time the minimum and maximum are increasing with growing energy.

3. The slope of differential cross section becomes small after the diffraction maximum. Its magnitude changes from 1.8 to 0.9 when $|t|$ changes from 3 to 14 GeV^2.

4. There is no another diffraction minimum up to $|t| \sim 14.2$ GeV^2.

Note should be made that different models of the Chow-Yang type [3], Regge eikonal models [4], and quasipotential models with a Gaussian quasipotential [5] cannot reproduce the picture of proton-proton scattering in such a large momentum-transfer region. Most of these models lead to the slope $b \sim b(0)/2 \sim$ $\sim$ 5-6 GeV^{-2} after the second maximum. They predict the second diffraction minimum at $|t| \sim$ 6-8 GeV^2; this is in contradiction with the available experimental data.

Some models can reproduce the main features of hadron-scattering in a wide momentum-transfer region (see, e.g., ref. [6]). Among the latter, we would like to point out the models based on the hypothesis of the composite structure [7-8] of interacting hadrons and on the Glauber representation for the scattering amplitude.

In the present paper we investigate the scattering of two spinless hadrons within a model of the eikonal type, which leads to one diffraction minimum only.

The eikonal representation for the scattering amplitude at small angles may be justified in the framework of the Logunov-Tavkhelidze quasipotential approach [9]. One can obtain the scattering amplitude as a power series in $\sqrt{s}$ using the smoothness hypothesis for the local quasipotential [1]

$$T(s,t) = T_0(s,t) + \frac{1}{2i\sqrt{s}} T_1(s,t) + O(\frac{1}{s}). \qquad (1)$$

Here the leading term of the scattering amplitude has the eikonal form

$$T_0(s,t) = is\int_0^\infty \rho\, d\rho\, J_0(\rho\Delta)(1-e^{i\chi(\rho,s)}) = is\int_0^\infty \rho\, d\rho\, J_0(\rho\Delta) f(\rho,s), \qquad (2)$$

where the eikonal phase $\chi(\rho,s)$ is connected with the quasipotential

$$\chi(\rho,s) = \frac{1}{s}\int_{-\infty}^{+\infty} V(\sqrt{\rho^2+z^2}, s)\, dz. \qquad (3)$$

Quasipotentials of the Gaussian type were used to analyse the experimental data on the quasipotential approach in a number of papers [12]. However, these quasipotentials lead to the amplitude which is an entire function of t; this is in contradiction with analytical properties [13].

It can be shown [14] that if the scattering amplitude satisfies the dispersion relations, the quasipotential can be represented as a superposition of Yukawa potentials

$$V(r,s) = \int_{\mu_0}^{\infty} d\mu \frac{e^{-\mu r}}{r} \rho(\mu,s). \qquad (4)$$

One of the possible kinds of these quasipotentials was suggested in ref. [15].

In order to investigate the hadron-hadron scattering in the wide momentum-transfer region , we shall use the local smooth

quasipotential which can be represented in the form (4). This type of quasipotentials can quantitatively reproduce all known properties of the scattering amplitude in the energy range $23.4 \le \sqrt{s} \le 62.1$ *GeV* and the t range $0 \le |t| \le 14.2$ *GeV*^{2} with the minimum number of free parameters.

DESCRIPTION OF THE MODEL

Let us consider the scattering of two hadrons in the asymptotic energy region. In this case we may retain only the leading asymptotic term of the scattering amplitude (2) omitting all correction terms in (1). We may take the main term of the eikonal phase in the form

$$\chi_0(\rho,s) = ihe^{-\mu\sqrt{b^2+\rho^2}} = i\delta_0(\rho,s). \qquad (5)$$

The parameters h , μ , b in (5) can change slowly with energy. The eikonal phase corresponds to the pure-umaginary quasipotential growing with energy as s . It may be verified that the quasipotential can be represented by (4).

The eikonal representation with the phase of type (5) was examined previously in the Chou-Yang model [16]. It was shown that the scattering amplitude reproduces the main properties of pp-scattering up to $|t| \sim 3$ *GeV*, it has only one diffraction minimum but diverges essentially with the experimental data for $|t| > 4\text{-}5$ *GeV*^{2}.

Let us consider, besides the usual elastic rescattering (*fig1*)

$$f_{el.} = -\sum_{n=1}^{\infty} (-\delta_0)^n / n!,$$

some possible inelastic effects with the particle beams in intermediate states (*fig. 2*). In this case we can change the sum over all intermediate states by two particles with some effective mass. As a result, f_{in} becomes

$$f_{in}(\rho,s) = -\gamma\delta_0^2(\rho,s).$$

(γ is some constant).

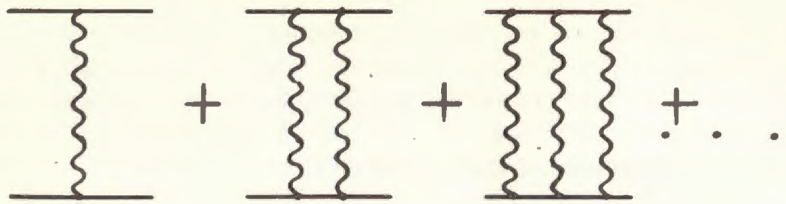

Fig. 1. Contribution of elastic rescattering to the scattering amplitude.

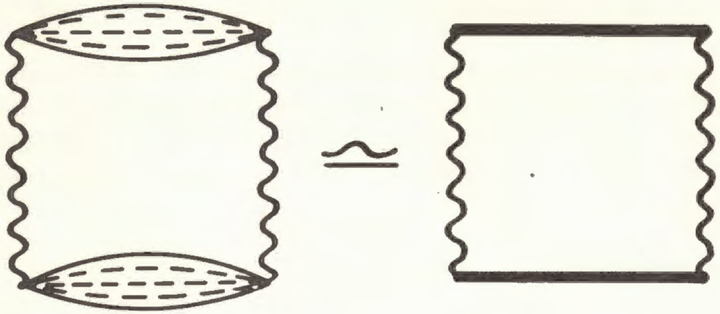

Fig. 2. Inelastic effects with forming particle beams in the s – channel.

Taking into account such inelastic effects, we can write the eikonal phase in the form

$$\delta(\rho, s) = \delta_0(\rho, s) - \gamma \delta_0^2(\rho, s). \tag{6}$$

The energy dependence of the quasipotential parameters can be determined by using the hypothesis of geometrical scaling[17], by which the whole energy dependence concentrates within the interaction range, and in our case only two parameters μ, b depend on energy, moreover, $\mu b = \text{const}$.

The slope of the diffraction peak and total cross sections are proportional to the b squared in the geometrical scaling approximation

$$\sigma_{tot} \sim B \sim b^2 .$$

If the total cross section grows with energy logarithmically, we obtain

$$b = b_0 \sqrt{1 + a \ln s} .$$

The real part of the scattering amplitude can be determined by using the local dispersion relations[18]:

$$\text{Re}\, T(s,t) = \frac{\pi}{2} \frac{d}{d \ln s} \text{Im}\, T(s,t), \tag{7}$$

which can be rewritten in terms of the eikonal phase

$$\text{Re}\, \chi(\rho, s) = \frac{\pi}{2} \frac{d}{d \ln s} \text{Im}\, \chi(\rho, s).$$

It is easy to see that the real part (7) is the first expansion term of the unique analytic function

$$\chi(\rho, s) = \chi(\rho, \ln s - i \frac{\pi}{2}).$$

As a result, the eikonal phase reads

$$\delta(\rho, s) = h(e^{-\mu\sqrt{b^2+\rho^2}} - \gamma h e^{-2\mu\sqrt{b^2+\rho^2}}), \tag{8}$$

where

$$h\gamma = \text{const}; \quad b = b_0 \kappa; \quad \mu = \mu_0/\kappa; \quad \kappa = \sqrt{1 + a(\ln s - \frac{i\pi}{2})}.$$

Below we shall use the eikonal phase formulae (8) for the analysis of the high energy pp -scattering experimental data in the wide t region.

One can represent the corresponding scattering amplitude in the explicit form. Here we shall write only the term corresponding to the pure-elastic rescattering ($\gamma = 0$)

$$T(s,t) = -\sum_{n=1}^{\infty} \frac{(-h)^n}{(n-1)!} \frac{\mu}{(n^2\mu^2+\Delta^2)^{3/2}} (1 + b\sqrt{n^2\mu^2+\Delta^2})\, e^{-b\sqrt{n^2\mu^2+\Delta^2}} ,$$

$$t = -\Delta^2. \tag{9}$$

It is easy to see that the scattering amplitude (9) is an analytic function of t. It has root branchpoints at $t = \mu^2, (2\mu)^2, (3\mu)^2 \ldots$

ANALYSIS OF EXPERIMENTAL DATA AND DISCUSSION OF RESULTS

We have analysed all the known pp -experimental data in the energy range $\sqrt{s} \geq 23.4$ *GeV* and $0 \leq |t| \leq 14.2$ GeV^2 . Parameters of the eikonal phase were determined by minimizing the χ^2 functional

$$\chi^2 = \sum_{ki} \frac{(F_i^k - M_k F_i^k(x_n))}{(\sigma_i^k)^2}, \tag{10}$$

where F_i^k is the experimental quantity measured at the i -th point of the k -th experiment, $F_i^k(x_n)$ is the theoretical value for the same point, σ_i^k, is the experimental error of F_i^k , M_k, the norm of the k -th experiment, that is the systematic error of the k -th experiment. We restrict the deviation of M_k from 1 to 8%. We calculated only three parameters h , μ_0 , b_0, which were related to the effective constant, effective mass, and effective radius of the central range of strong interaction, from the fit of experimental data.

The quantity γh was chosen equal to unity. The coefficient $a = 0.075$ was fitted from the new experimental data for the total cross section [19]. This value is approximately equal to that from [20].

The best description of experimental data ($\chi^2 = 541$*, $\overline{\chi^2} = 449$, $\chi^2/\overline{\chi^2} = 1.205$) corresponds to the following three parameters

$$h = 4.96 \pm 0.02,$$

$$\mu_0 = (0.66 \pm 0.005)\ \mathrm{GeV},$$

$$b_0 = (1.875 \pm 0.005)\ \mathrm{GeV}^{-1}.$$

The norm coefficients M_k are shown in the *table*. Note that a sufficiently good description of experimental data can be obtained without the norms

$$\chi^2/\overline{\chi^2} = 1.45 .$$

---

* We neglect the points exceeding three standard deviations from the fit.

The calculated results are compared with experimental data in *Figs. 3,4*. It is easy to see that the theoretical results reproduce all specific features of the differential cross section in the wide momentum-transfer region. The accurate values for the differential cross section minimum and maximum and the predictions for the range $|t| = 20$ GeV^2 are shown in the *table*. The obtained total cross section is in good agreement with the results of ref. [19] (see the *table*).

Table

$\sqrt{s}$	23.5	30.6	44.7	52.8	62.I	200
$M_K^{exp.}$	0.92	0.92	0.96	I.08	I.0I8	
$\|t\|_{min.}^{exp.}$	I.44± 0.03	I.4I8± 0.003	I.370± 0.005	I.348± 0.006	I.322± 0.0I2	
$\|t\|_{min}^{theor.}$	I.47	I.43	I.38	I.35	I.33	I.20
$\|t\|_{max}^{exp.}$	I.97± 0.003	I.93± 0.003	I.92± 0.I0	I.8I± 0.07	I.8I 0.07	
$\|t\|_{max}^{theor.}$	I.9I	I.89	I.8	I.77	I.73	I.60
$\frac{d\sigma}{dt}\Big\|_{max}^{exp.} \times 10^5$	4.5± 0.3	4.2± 0.3	5.2± 0.3	5.8± 0.5	6.3± 0.5	
$\frac{d\sigma}{dt}\Big\|_{max}^{theor.} \times 10^5$	4.9	5.22	5.5	5.8	6.0	7.I
$\frac{d\sigma}{dt}\Big\|_{\|t\|=20.}^{theor.} \times 10^{13}$	I9.3	I5.03	I0.72	9.22	7.98	2.9
$\sigma_{tot}^{exp.}$	39.0I± 0.29	40.35± 0.34	4I.45± 0.26	42.38± 0.29	43.05± 0.33	
$\sigma_{tot}^{theor.}$	39.02	40.08	4I.58	42.23	42.87	
$B_{\|t\|=20.}$ slope	0.55	0.56	0.57	0.575	0.58	0.6

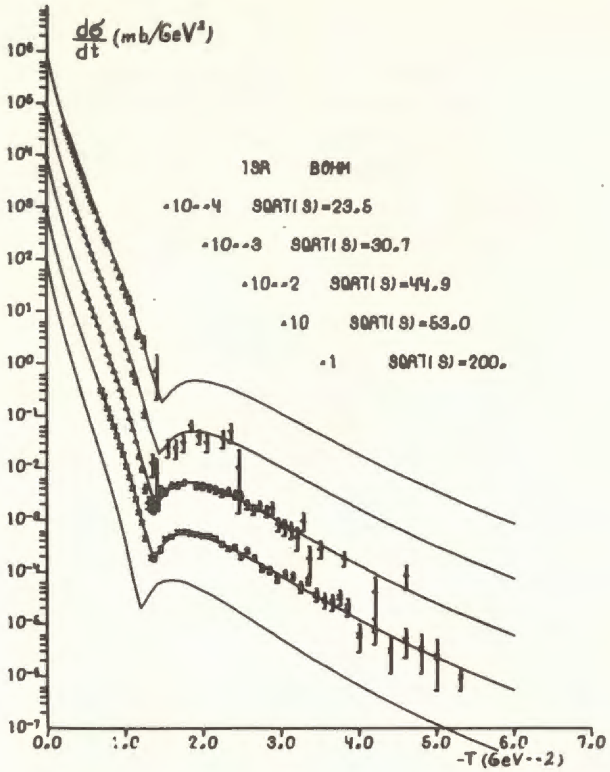

Fig. 3. Calculated differential cross sections at different energies. Data are from paper by A.Bohm et al.[1]. *Predictions are given for* $\sqrt{s} = 200$ *GeV.*

The differential cross section for the pp scattering at $\sqrt{s} = 200$ *GeV* is shown in *fig. 3*. In *fig.5* the predictions for the small $|t| \leq 0.4$ GeV^2 region together with the data[21] are plotted. Our model predicts the smooth decrease of the slope of the diffraction peak with increasing momentum transfer. The average values of the slope are equal to $\bar{b} = 14.2$ $(0 < |t| \leq 0.15)$ and to $\bar{b} = 11.3$ $(0.15 < |t| \leq 0.4)$ for the energy $\sqrt{s} = 52.8$ *GeV*.

From *fig. 7* one can see that the theoretical curve reproduces not only the accelerator data[22–24] but also the cosmic data on total cross sections[25].

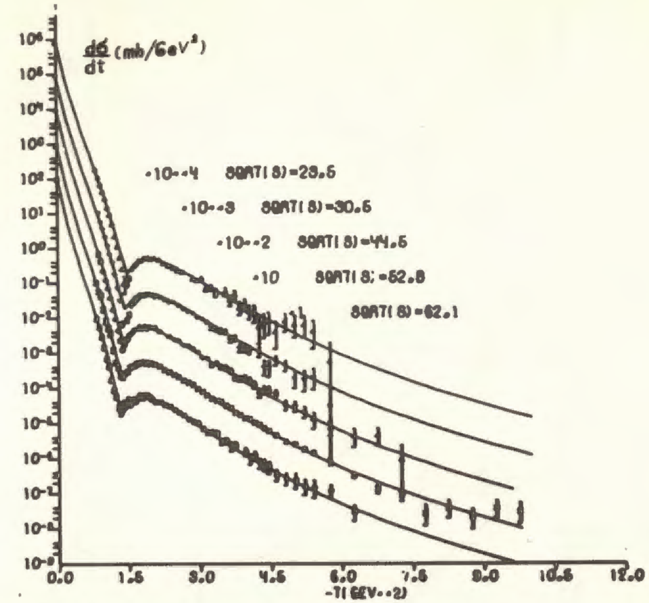

Fig. 4. Calculated differential cross sections at different energies. Data from paper by E.Nagy et al.[2].

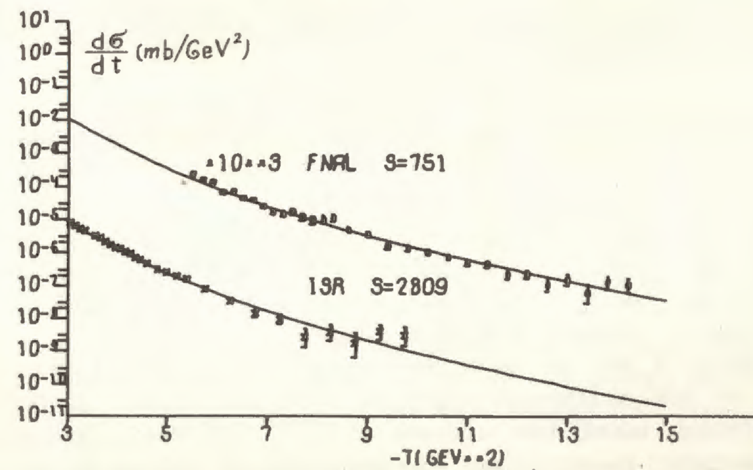

Fig. 5. Behaviour of differential cross sections at large transfer momenta. Data from papers[20,b].

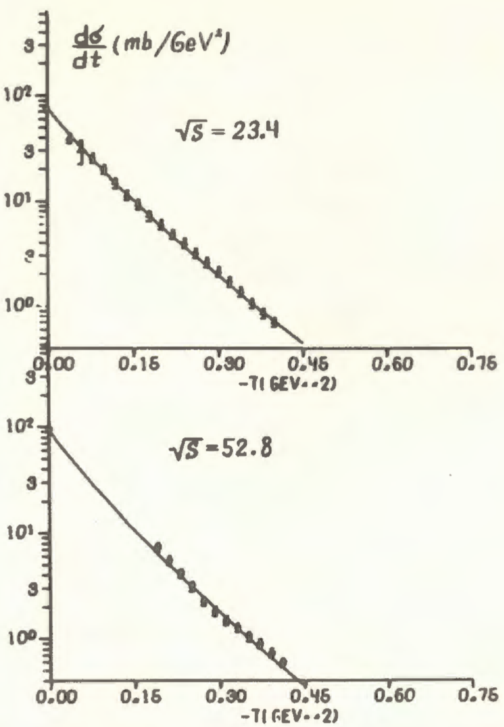

Fig. 6. The model predictions for small momentum transfers. Comparison is made with data from ref. [21].

Our predictions for the slope of differential cross sections in a wide momentum transfer region is shown in *Fig. 8* for the energy $\sqrt{s} = 23.4$ and $\sqrt{s} = 52.8$ *GeV*.

For $\sqrt{s} = 52.8$ the slope changes slowly at small $|t|$ up to $b \approx 9.7$ at $|t| \approx 0.67$. Near the diffraction minimum ($|t| \approx 1{,}23$) the slope grows up to $b = 15.3$ and smoothly changes from 0.87 to 0.57 when $|t|$ changes from 10 to 20 GeV^2.

Figures 9 and *10* show the curves for imaginary and real parts of the scattering amplitude with and without inelastic rescattering taken into account at $\sqrt{s} = 52.8$ *GeV*. It is seen that inelastic rescatterings are important at sufficiently large momentum transfer $|t| \sim 0.8$-1 GeV^2. However, by taking it into account, the scattering amplitude has the same qualitative behaviour. Its imaginary part has only one zero and its real

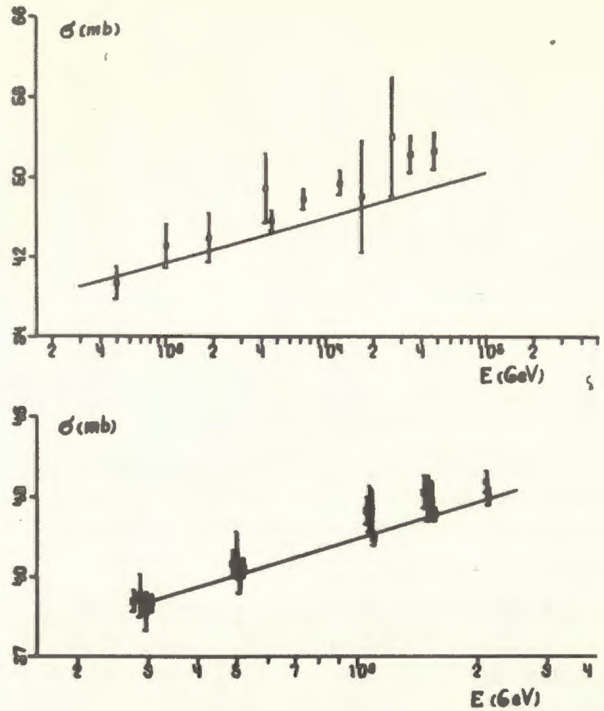

Fig. 7. The energy dependence of the calculated total cross sections (the bottom part shows accelerator data [19,22-24] *, the top part, the cosmic data* [25] *).*

part has two zeros. This may be due to the use of the local dispersion relations for the real part of the scattering amplitude [20].

The imaginary part of the scattering amplitude is five to ten times as large as the real part in the whole momentum-transfer region except the diffraction minimum point. So it gives the main contribution to the amplitude. The effective radius of the central part of the interaction region is approximately half of the hadron radius. It grows with energy as $\sqrt{\ln s}$ and increases from 0.45 to 0.48 *fm* when energy $\sqrt{s}$ changes from 23 to 60 *GeV*.

Thus, taking into account the analytical properties of the scattering amplitude we have formulated the model quantitatively describing all known experimental data in the spinless case.

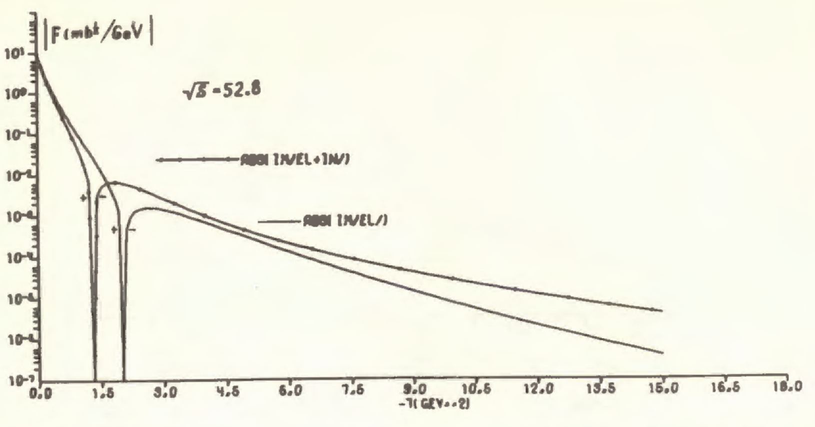

Fig. 8. The absolute value of the imaginary part of the scattering amplitude for $\sqrt{s}$ = *52.8 GeV. (–·–·– with and —— without the contributions from inelastic rescatterings).*

However, the spin effect may play a certain role at high energies and large momentum transfers [6]. So, it is very important to investigate the spin effects in proton-proton scattering in the energy range $p_L \geq$ 200-400 *GeV/c* and $|t| \geq 3$ *GeV*^{2}.

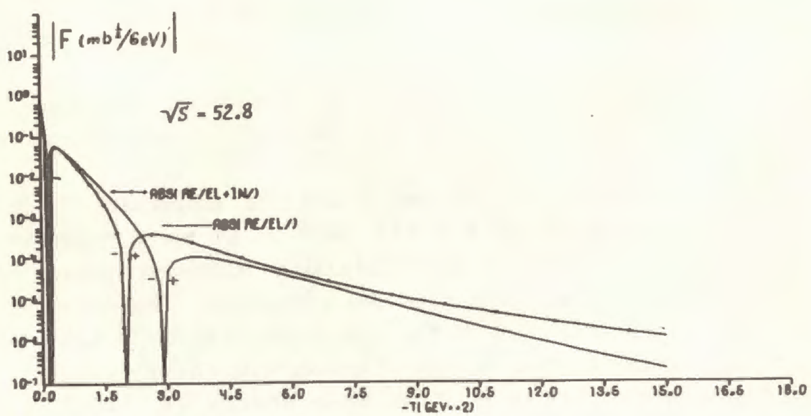

Fig. 9. The absolute value of the real part of the pp *-scattering amplitude calculated within our model for* $\sqrt{s}$= *52.8 GeV (–·–· with and —— without the contributions from inelastic scatterings).*

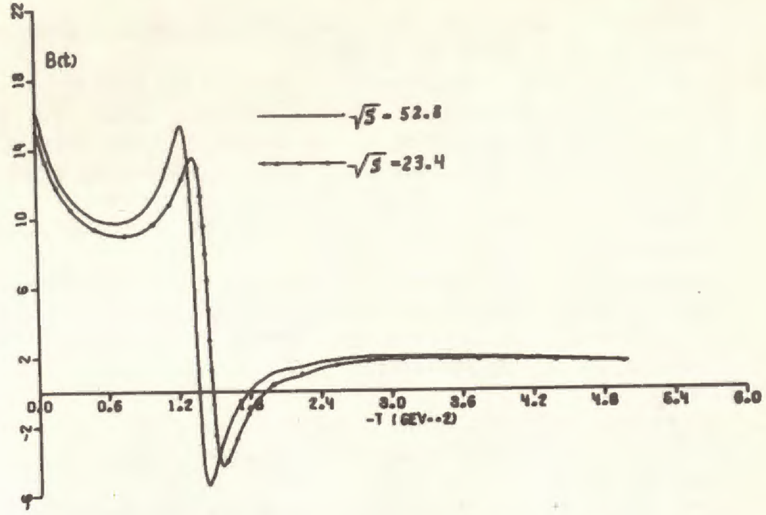

Fig. 10. Predictions for the slope $B(t) = \frac{d}{dt}(\ln(\frac{d\sigma}{dt}))$ *for energies* —— $\sqrt{s}$ = *52.8 GeV and – · –* $\sqrt{s}$*=23.4 GeV.*

It is interesting to note that differential cross sections change approximately by four orders in the momentum range 4 *GeV*$^2 < |t| < 12$ *GeV*^{2}. At the same time it changes only by one and one half-two orders when $|t|$ changes from 12 to 20 *GeV*^{2}. It is very important to experimentally check this prediction of our model.

The authors express their deep gratitude to V.A.Matveev, A.N.Tavkhelidze for interest in the work and useful remarks. We thank also A.V.Koudinov, V.K.Mitrjushkin, S.V.Rusakov , M.A.Smondyrev, V.A.Tsarev for fruitful discussions.

REFERENCES

1. *Bohm A. et al. Aachen - CERN - Geneva - Harvard - Torino Collaboration. Phys.Lett., 1974, 49B, p.491.*
2. *a) Nagy E. et al. CETN - Geneva - Switzerland - Hamburg - Heidelberg - Annecy - Wien. Nucl.Phys., 1979, B150, p.221.*

b) Cdnetti S. et al. Cornell - McGill - Moskow Collaboration. Phys.Rev.Lett., 1978, 41, p.924.
4. Chow T.T., Yang C.N. Phys.Rev., 1968, 170, p.1591.
Durand L., Lipes R.G. Phys.Rev.Lett., 1968, 20, p.637.
4. Frautschi S., Margolis B. Nuovo Cimento, 1968, 56A, p.1155.
5. Garsevanishvili V.R., Matveev V.A., Slepchenko L.A. Particles and Nuclei. Atomizdat, M., 1970, v.1, p.92.
6. Tsarev V.A. Rapporteur's talk at the XIX Int. Conf. on High Energy Phys., Tokyo, 1978.
7. Wakaizumi S., Tanimoto M. Phys.Lett., 1977, 70B, p.55.
Bialas A. et al. Acta Phys. Pol., 1977, B8, p.855.
8. Goloskokov S.V. et al. JINR, E2-12565, Dubna, 1979.
9. Logunov A.A., Tavkhelidze A.N. Nuovo Cim., 1963, 29, p.380.
10. Garsevanishvili V.R. et al. TMF, 1971, 6, p.36.
11. Alliluyev S.P., Gershtein S.S., Logunov A.A. Phys.Lett., 1965, 18, p.195.
Logunov A.A., Khrustalev O.A. Particles and Nucleus. Atomizdat, M., 1970, v.1., p.72.
12. Garsevanishvili V.R. et al. Phys.Rev., 1971, D4, p.849.
Dzhgarkava M.I. et al. Nucl.Phys., 1973, B67, p.232.
Nucl.Phys., 1974, B79, p.396. JINR, E2-10971, Dubna, 1977.
13. Logunov A.A., Mestvirishvili M.A. Phys. Lett., 1967, 24B, p.620.
Mestvirishvili M.A., Rcheulishvili G.L. Yad. fiz., 1970, 11, p.688.
14. Filippov A.T. In Winter School on Theoretical Physics in JINR, Dubna, 1964, v.2, p.80.
15. MestvirishviliM.A., Rcheulishvili G.L. TMF, 1971, 8, p.206.
16. Cheng H., Walker J., Wu T.T. Phys.Lett., 1973, 44B, p.97.
17. Dias de Deus I. Nucl.Phys., 1973, B59, p.231.
Buras A.I., Dias de Deus I. Nucl.Phys., 1974, B71, p.481.
18. Bronzan I.B. et al. Phys.Lett., 1974, 49B, p.272.
19. Amaldi U. et al. Phys.Lett., 1975, 62B, p.460.
20. Barger V. et al. Nucl.Phys., 1975, B88, p.237.
21. Kwah N. et al. Phys.Lett., 1975, 58B, p.233.
22. Amendolina S.R. et al. Phys.Lett., 1973, 44B, p.119.
23. Amaldi U. et al. Phys.Lett., 1973, 44B, p.112.
24. Eggert H. et al. Nucl.Phys., 1975, B98, p.93.
25. Yodh G.B. Prospects of Strong Interaction at Isabelle., 1977, p.47, Brookhaven, New York, 1977.

Received by Publishing Department on June 29 1979.